LaBaNiO$_4$: a Fermi glass

LaBaNiO$_4$: a Fermi glass

A Schilling[1,5]**, R Dell'Amore**[1]**, J Karpinski**[2]**, Z Bukowski**[2]**,
M Medarde**[3,4]**, E Pomjakushina**[3,4] **and K A Müller**[1]

[1] Physics Institute of the Universität of Zürich, Winterthurerstrasse 190, CH-8057 Zürich,
Switzerland
[2] Laboratory for Solid-State Physics, ETH Zürich HPF F-7, CH-8093 Zürich, Switzerland
[3] Laboratory for Neutron Scattering, ETHZ and PSI, CH-5232 Villigen PSI, Switzerland
[4] Laboratory for Developments and Methods, ETHZ and PSI, CH-5232 Villigen PSI,
Switzerland

E-mail: schilling@physik.uzh.ch

Abstract
Polycrystalline samples of LaSr$_{1-x}$Ba$_x$NiO$_4$ show a crossover from a state with metallic
transport properties for $x = 0$ to an insulating state as $x \to 1$. The end member LaBaNiO$_4$ with
a nominal nickel Ni 3d^7 configuration might therefore be regarded as a candidate for an
antiferromagnetic insulator. However, we do not observe any magnetic ordering in LaBaNiO$_4$
down to 1.5 K, and despite its insulating transport properties several other physical properties of
LaBaNiO$_4$ resemble those of metallic LaSrNiO$_4$. Based on an analysis of electrical and
thermal-conductivity data as well as magnetic-susceptibility and low-temperature specific-heat
measurements, we suggest that LaBaNiO$_4$ is a Fermi glass with a finite electron density of
states at the Fermi level but these states are localized.

(Some figures in this article are in colour only in the electronic version)

1. Introduction

Certain transition-metal oxides show unique physical properties that are not only of academic interest but also make them technologically useful. The discoveries of high-temperature superconductivity [1] and colossal magnetoresistance [2] in such oxides have triggered tremendous activity in the research into these compounds with the aim of understanding their peculiar magnetic and transport properties.

The metallic state in the high-temperature superconductors, for example, is highly unusual because it evolves from originally electrically insulating oxides. Stoichiometric La$_2$CuO$_4$ is antiferromagnetic near room temperature, with copper in a Cu 3d^9 (spin $S = 1/2$) configuration, and it is regarded as a Mott insulator. These features are generally believed to be important ingredients for the occurrence of superconductivity on subsequent doping of the compound with hole-type charge carriers, e.g. by the partial substitution of La by Ba or Sr [1]. In contrast, stoichiometric LaSrNiO$_4$, which shares the same K$_2$NiF$_4$ structure with La$_2$CuO$_4$, is metallic [3], although a 3d^7 configuration of nickel in a low-spin $S = 1/2$ state might be expected that could also lead

to an antiferromagnetic and insulating state. This fact has been explained with the partial occupation of the oxygen O 2p energy band of LaSrNiO$_4$ by hole states that hybridize with the nickel Ni 3d^8 states, in contrast to La$_2$CuO$_4$ which shows a completely filled copper Cu 3d^9 lower-Hubbard band [4]. The occupation of oxygen 2p hole states, leaving the nickel in an Ni 3d^8 configuration, is very common in nominally trivalent-nickel oxides [5–7]. For this reason LaSrNiO$_4$ has not been considered as a serious candidate for a 'parent compound' of superconductors, and substitution experiments in La$_{2-y}$Sr$_y$NiO$_4$ over a wide range of doping (i.e. $0 \leqslant y \leqslant 1.5$) have not resulted in superconducting samples [3, 8].

In great contrast to the metallic character of LaSrNiO$_4$, the isostructural compound LaBaNiO$_4$ has been reported to be an insulator at zero temperature T, and to undergo a transition from a high-spin to a low-spin $S = 1/2$ state of Ni around $T \approx 120$ K with decreasing temperature [9]. It is therefore of particular interest to study the influence of a partial or a complete substitution of Sr by Ba in LaSrNiO$_4$ on the physical properties that are expected to be affected by a resulting stretching of the crystal lattice [9, 10]. We have found that there exists a solid solution of Ba in LaSr$_{1-x}$Ba$_x$NiO$_4$ for $0 \leqslant x \leqslant 1$, and we have measured the electrical and the thermal

---

[5] Author to whom any correspondence should be addressed.

1

conductivities, the magnetic susceptibilities and the low-temperature specific heats of polycrystalline $LaSr_{1-x}Ba_xNiO_4$ samples. Since possible magnetic-ordering phenomena as well as other physical properties may strongly depend on the exact oxygen stoichiometry, we have combined a thorough neutron-diffraction analysis of the end member $LaBaNiO_4$ with a chemical analysis and with additional heat-treatment experiments at an elevated oxygen pressure.

2. Experimental details

We have prepared polycrystalline samples of $LaSr_{1-x}Ba_xNiO_4$ for $x = 0$, 0.25, 0.3, 0.35, 0.4, 0.45, 0.5, 0.75 and 1.0 by a standard wet chemical procedure. Mixtures of corresponding metal nitrates were dissolved in nitric acid. The liquid was then slowly evaporated, and the remaining mixture of nitrate powders was pre-reacted at $900\,°C$ for several hours in air. The remaining mixture of oxides was pressed into pellets and sintered at $1100\,°C$ for 3 days in air. Samples of $LaSr_{0.5}Ba_{0.5}NiO_{4-\delta}$ ($x = 0.5$) and $LaBaNiO_{4-\delta}$ ($x = 1.0$) were post-annealed at temperatures between 400 and $600\,°C$ and at an O_2 pressure of 500–880 bar (50–88 MPa). After testing the phase purity of all the samples with a Guinier camera using $Cu\,K\alpha_1$ radiation we have performed a thermogravimetric analysis on 100 mg of each as-prepared and high-pressure oxygen-annealed $LaBaNiO_{4-\delta}$, followed by neutron-diffraction experiments on 5 g powdered samples of the same batches at various temperatures between 1.5 and 550 K. These experiments were performed at the neutron source SINQ in Villigen, Switzerland, on the high resolution neutron powder diffractometer (HRPT) ($\lambda = 0.15$ and 0.18 nm) and the cold neutron powder diffractometer (DMC) ($\lambda = 0.245$ and 0.4 nm). The four-probe electrical conductivities and the AC magnetic susceptibilities were measured for all the samples in zero DC magnetic field. Specific-heat data were taken on three samples ($x = 0$ and high-pressure oxygen-annealed $x = 0.5$ and 1), while the thermal conductivities were measured only on the $x = 0$ and the high-pressure oxygen-annealed $x = 1$ samples. All the physical properties were collected using standard factory options in a commercial PPMS platform (Physical Property Measurement System, Quantum Design Inc., San Diego, USA).

3. Results

3.1. Chemical analysis and neutron-diffraction experiments

A thermogravimetric analysis of the as-prepared $x = 1$ sample $LaBaNiO_{4-\delta}$ yielded an oxygen content 3.85(1) ($\delta \approx 0.15$) assuming a nominal cation ratio La:Ba:Ni = 1:1:1. Under the same assumption, a Rietveld refinement of the room-temperature neutron-diffraction pattern using the space group $I4/mmm$ proposed in previous work [9, 10] (see figure 1) also gave an oxygen content 3.85(1), with oxygen vacancies located both in the apical positions ($\approx 33\%$) and in the basal planes ($\approx 66\%$). A refinement with the restriction $(La + Ba):Ni = 2:1$ gave similar R-factors and suggested a composition $La_{1.27(2)}Ba_{0.73(2)}NiO_{3.97(2)}$ which would imply a

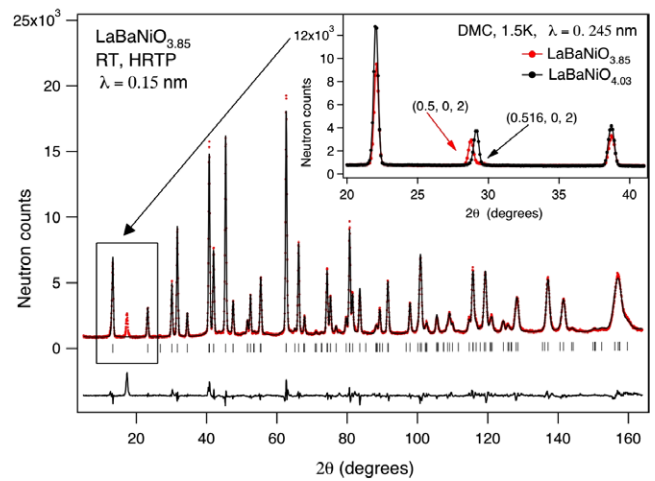**Figure 1.** Neutron-powder-diffraction pattern of $LaBaNiO_{3.85}$ taken at room temperature, together with a Rietveld-refinement fit using the space group $I4/mmm$. The inset shows the displacement of the $(1/2, 0, 2)$ Bragg reflection to the incommensurate position $(0.516, 0, 2)$ upon increasing the oxygen content to 4.025.

Table 1. Lattice parameters and refined atomic coordinates of $LaBaNiO_4$ using the space group $I4/mmm$. (La, Ba): 4e ($0\ 0\ z_1$); Ni: 2a ($0\ 0\ 0$); O1: 4e ($0\ 0\ z_2$); O2: 4c ($0.5\ 0\ 0$).

	$T = 1.5$ K	295 K	550 K
a (nm)	0.384 970(11)	0.385 519(11)	0.386 754(11)
c (nm)	1.273 670(56)	1.278 893(57)	1.286 938(58)
z_1	0.360 86(62)	0.360 50(63)	0.360 80(64)
z_2	0.164 97(57)	0.165 09(59)	0.165 68(58)

considerable amount of unreacted BaO present as an impurity. However, we could not find any detectable amount of BaO and/or its carbonated subproducts, either in the diffraction patterns or by chemical methods. To clarify this issue we repeated the chemical analysis and the neutron-diffraction measurements on samples that were annealed at $400\,°C$ under an oxygen pressure of 880 bar (88 MPa) for 50 h (annealing at $600\,°C$ at elevated oxygen pressure resulted in a partial decomposition of the sample). According to the observed weight change we estimated an oxygen uptake of ≈ 0.16/f.u. during this procedure, which is consistent with the above value $\delta \approx 0.15$ for the as-prepared sample. The thermogravimetric analysis of the high-pressure oxygen-annealed sample resulted in an oxygen content 4.025(10), thereby confirming the nearly stoichiometric composition $LaBaNiO_4$ after the high-oxygen pressure treatment. The structural parameters of oxygen-annealed $LaBaNiO_4$ as obtained from DMC data refinements ($\lambda = 0.245$ nm) using the tetragonal space group $I4/mmm$ are listed in table 1 for three different temperatures $T = 1.5$ K, 295 K and 550 K, respectively.

As expected and also reported in [9, 10], the lattice parameters of $LaBaNiO_4$ are larger than those of $LaSrNiO_4$ ($a = 0.3826$ nm, $c = 12.45$ nm [11]), and vary smoothly from $x = 0$ to 1 according to our Guinier $Cu\,K\alpha_1$ diffraction patterns. In agreement with a report by Alonso *et al* [10] we detected a distinct extra reflection peak in the neutron-diffraction data of the as-prepared $LaBaNiO_{4-\delta}$ sample that
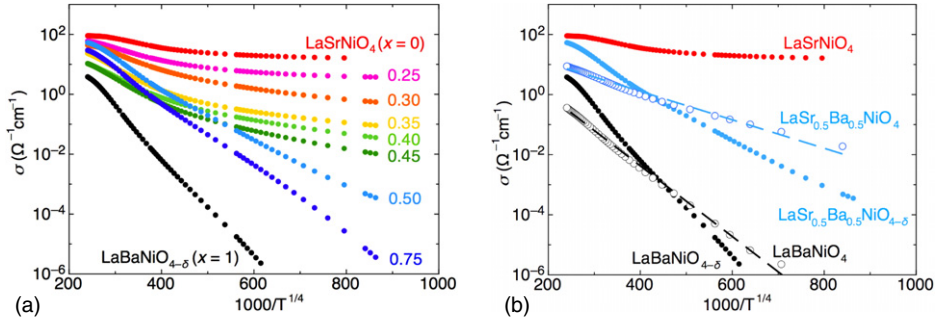
Figure 2. (a) Electrical conductivities σ versus $T^{-1/4}$ of as-prepared samples (full circles) and (b) of high-pressure oxygen-annealed samples (open circles). The dashed lines are fits according to a variable-range hopping-type conductivity, see text.

can be indexed as (1/2, 0, 2), indicating a doubling of the unit cell in the a-direction and changing the crystal symmetry from tetragonal to orthorhombic. Upon high-pressure oxygen annealing, this peak slightly moved to an incommensurable position (0.516, 0, 2), see figure 1, and corresponding tiny higher-order peaks could also be indexed with a propagation vector $\boldsymbol{k} = (0.516, 0, 0)$. Since these peaks have not been observed in the x-ray diffraction patterns they could, in principle, be ascribed to the ordering of La/Ba [10] or they might even be of magnetic origin. This latter hypothesis can be safely excluded, however, since we did not observe any change in the respective peak intensities between 1.5 and 550 K. As the low-temperature oxygen treatment mainly affects the oxygen stoichiometry, the extra peak could also be ascribed to some kind of oxygen-vacancy and/or charge/stripe-ordering phenomenon, at least in the case of the oxygen-defective sample [12–14]. For stoichiometric LaBaNiO$_4$ with a nominally single-valent Ni^{3+}, this explanation does not seem to be very plausible, however. Another possibility that could explain the very similar intensities of the extra peak in both the as-prepared and the oxidized samples is the existence of a charge-density wave of the type Ni$^{3+\delta}$/Ni$^{3-\delta}$. Such a charge disproportionation, although difficult to observe with diffraction techniques, has been recently reported for other stoichiometric Ni^{3+} compounds close to the boundary between localized and itinerant behaviour, such as AgNiO$_2$ [15] and YNiO$_3$ [16]. In the present LaBaNiO$_{3.85}$ and LaBaNiO$_4$ samples, however, we have not yet been able to establish a model for a charge and/or an oxygen-vacancy ordering that could sufficiently reproduce the observed intensity of the observed extra peak.

It is important to mention that apart from the displacements of the Bragg reflections due to thermal dilatation, the diffraction patterns for fully oxygenated LaBaNiO$_4$ at different temperatures look *exactly the same*. In particular there is no evidence for the appearance of additional reflections at low temperatures that would suggest any type of magnetic order in LaBaNiO$_4$.

3.2. Electrical conductivity

In figure 2(a) we show the electrical conductivities of the as-prepared samples, plotted as σ versus $T^{-1/4}$ on a semi-logarithmic scale. The measured data for LaSrNiO$_4$, with a

slight decrease of σ with decreasing temperature, are perfectly in line with corresponding data from the literature [3, 8]. As a general trend, the low-temperature conductivity decreases with increasing Ba content, but more importantly, its temperature dependence changes from a relatively weak one for LaSrNiO$_4$ ($x = 0$) to a $\sigma(T)$ that varies over more than six decades from room temperature down to $T = 7$ K for LaBaNiO$_{4-\delta}$ ($x = 1$). In figure 2(b) we show the corresponding data of the samples that have been annealed at an elevated oxygen pressure. Although there is a change in the data of LaSr$_{0.5}$Ba$_{0.5}$NiO$_{4-\delta}$ and LaBaNiO$_{4-\delta}$ upon oxygen annealing, namely a decrease in the room-temperature conductivity and slight flattening of $\sigma(T)$, the strongly temperature dependent character of the electrical conductivity remains, confirming that stoichiometric LaBaNiO$_4$ is an insulator at $T = 0$. As was already noticed by Demazeau *et al* [9] the best physically reasonable fit to the $\sigma(T)$ data of LaBaNiO$_{4-\delta}$ is according to a strongly T-dependent 3D variable-range hopping-type (VRH) conductivity, $\sigma(T) = \sigma_0 \exp[-(T_0/T)^{1/4}]$ [17] (see dashed lines in figure 2(b)), which we will discuss later in section 4.

In the following we will restrict our discussion of the other measured physical properties to the samples LaSrNiO$_4$, the oxygen treated LaSr$_{0.5}$Ba$_{0.5}$NiO$_4$ (as a prototype of an intermediate composition) and LaBaNiO$_4$ to avoid unnecessary complications coming from an off-stoichiometric oxygen content.

3.3. Magnetic susceptibility

In figure 3 we present the magnetic-susceptibility $\chi(T)$ data of LaSrNiO$_4$ and oxygen treated LaSr$_{0.5}$Ba$_{0.5}$NiO$_4$ and LaBaNiO$_4$. Despite the large differences in the respective electrical conductivities, the three curves all look very similar, with an almost constant χ_0 at high temperatures and a small Curie-like upturn in $\chi(T)$ at low temperatures, which is in agreement with the data for LaSrNiO$_4$ from the literature [3]. A corresponding fit to the data above $T = 40$ K assuming $\chi(T) = C/T + \chi_0$ gives an almost universal value $\chi_0 \approx 4 \times 10^{-4}$ emu mol^{-1} and a Curie term C of the order of 1– 2×10^{-2} emu K mol^{-1} (see table 2), which corresponds to only about 5% of the value for free low-spin $S = 1/2$ Ni^{3+} ions. This indicates that the magnetic moments of Ni in electrically insulating LaBaNiO$_4$ are in a large majority *not localized*. A mathematically better fit to all the data, including
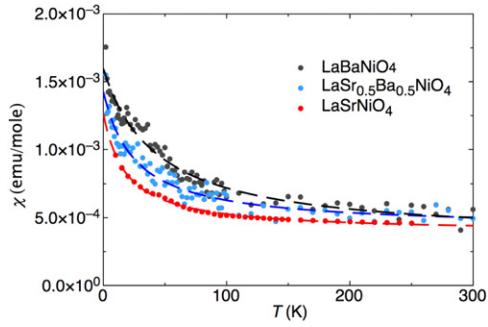
Figure 3. Magnetic susceptibilities $\chi(T)$ of LaSrNiO$_4$ (bottom), oxygen treated LaSr$_{0.5}$Ba$_{0.5}$NiO$_4$ (middle) and LaBaNiO$_4$ (upper curve). The dashed lines are fits to the data assuming $\chi(T) = C/(T + \Theta) + \chi_0$ (see text and table 2).
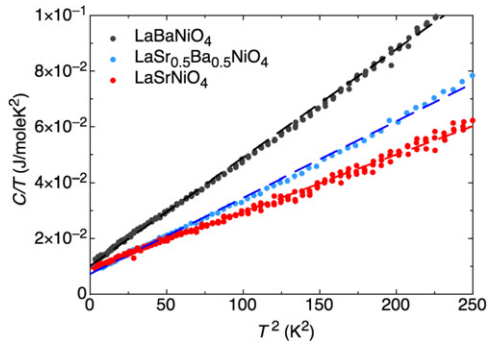

Figure 4. Reduced specific-heat C/T versus T^2 data of LaSrNiO$_4$ (bottom), oxygen treated LaSr$_{0.5}$Ba$_{0.5}$NiO$_4$ (middle) and LaBaNiO$_4$ (upper curve). The dashed lines are fits to $C(T) = \beta T^3 + \gamma T$ (see text and table 3).

Table 2. Fitting results of the $\chi(T)$ data shown in figure 3. The first row for each compound corresponds to a fit according to $\chi(T) = C/T + \chi_0$, the second row to $\chi(T) = C/(T + \Theta) + \chi_0$.

	C (emu K mol^{-1})	χ_0 (emu mol^{-1})	Θ (K)
LaSrNiO$_4$	$1.10(2) \times 10^{-2}$	$4.12(2) \times 10^{-4}$	—
	$1.62(7) \times 10^{-2}$	$3.90(5) \times 10^{-4}$	18.4 ± 1.3
LaSr$_{0.5}$Ba$_{0.5}$NiO$_4$	$1.60(11) \times 10^{-2}$	$4.57(15) \times 10^{-4}$	—
	$2.58(30) \times 10^{-2}$	$4.23(21) \times 10^{-4}$	25.7 ± 3.2
LaBaNiO$_4$	$2.41(10) \times 10^{-2}$	$4.49(13) \times 10^{-4}$	—
	$5.40(60) \times 10^{-2}$	$3.41(31) \times 10^{-4}$	43 ± 5

Table 3. Fitting results from the specific-heat data in figure 4 according to $C(T) = \beta T^3 + \gamma T$.

	LaSrNiO$_4$	LaSr$_{0.5}$Ba$_{0.5}$NiO$_4$	LaBaNiO$_4$
β (mJ mol^{-1} K^{-4})	0.204(1)	0.273(1)	0.388(1)
Θ_{D} (K)	405	368	327
γ (mJ mol^{-1} K^{-2})	9.15(11)	7.27(16)	10.1(1)

for LaSr$_{0.5}$Ba$_{0.5}$NiO$_4$ and even for insulating LaBaNiO$_4$, which is rather surprising. The measured Sommerfeld coefficients $\gamma \approx$ 7–10 mJ mol^{-1} K^{-2} are all of the same order of magnitude as in metallic LaNiO$_3$ ($\gamma \approx 13$ mJ mol^{-1} K^{-2} [18]) but they are large when compared to the free-electron value $\gamma \approx 2.0$ mJ mol^{-1} K^{-2} assuming one charge carrier per formula unit. In section 4 we will relate the measured Sommerfeld coefficients with the corresponding values for the Pauli-paramagnetic susceptibilities χ_0 and the respective free-electron values.

3.5. Thermal conductivity

In section 3.2. we have shown that the electrical transport in LaBaNiO$_4$ is far from being metallic. However, from the magnetic-susceptibility and the specific-heat data alone one cannot distinguish between the physical properties of LaSrNiO$_4$ and those of LaSr$_{0.5}$Ba$_{0.5}$NiO$_4$ and LaBaNiO$_4$, all resembling those of a metal. We therefore carried out additional thermal-conductivity measurements on LaSrNiO$_4$ and LaBaNiO$_4$ to probe a further transport property. As can be seen in figure 5, the thermal conductivity of LaSrNiO$_4$ is somewhat larger than that of LaBaNiO$_4$. To be able to make a fair comparison we make use of the kinetic expression for the lattice contribution to the thermal conductivity, $\lambda_{\mathrm{latt}} = C_{\mathrm{latt}} v l / 2$, where C_{latt} is the lattice specific heat per unit volume, v is the phonon group velocity and l is the phonon mean free path. Since v depends, to a first approximation, on the density ρ of a material as $\rho^{-1/2}$, we have to compare the quantities $C_{\mathrm{latt}} \rho^{-1/2} l$ to obtain an estimate for the respective lattice contributions. To calculate C_{latt} over the entire temperature range we have used the standard expression for a Debye solid using the above values for Θ_{D}, and used the x-ray densities $\rho = 6360$ kg m^{-3} for LaSrNiO$_4$ and $\rho = 6980$ kg m^{-3} for LaBaNiO$_4$, respectively.

Such a comparison is expected to work best in the high-temperature limit where we may assume that for a given temperature the phonon mean free path l is approximately the same in both isostructural compounds, while l is expected

those at temperatures below 40 K, is obtained by allowing for a Néel-type expression $\chi(T) = C/(T + \Theta) + \chi_0$, see figure 3. However, the qualitative results, namely a χ_0 of the order of 3–5 $\times 10^{-4}$ emu mol^{-1} and a fairly small Curie term, remain the same. Note that the free-electron value for the Pauli-paramagnetic susceptibility of a metal is $\chi_0 \approx 4 \times 10^{-5}$ emu mol^{-1} assuming one charge carrier per formula unit. The observed strong enhancement of the measured χ_0 values over the free-electron value will be discussed below in section 4.

3.4. Specific heat

In figure 4 we have plotted the specific-heat data of LaSrNiO$_4$, LaSr$_{0.5}$Ba$_{0.5}$NiO$_4$ and LaBaNiO$_4$ as C/T versus T^2 and for temperatures $T < 16$ K. A standard analysis accounting for a phonon contribution βT^3 and a linear term γT that is usually ascribed to a finite electron density of states at the Fermi level, gives the parameters presented in table 3. As expected from Debye theory, the Debye temperature $\Theta_{\mathrm{D}} = (233.8 n R / \beta)^{1/3}$ (with n the number of atoms per unit cell and the gas constant $R = 8.314$ J mol^{-1} K^{-1}) decreases for increasing molar mass, i.e. increasing Ba content. While the presence of a linear term in the specific heat of LaSrNiO$_4$ is not unexpected because of its metallic nature, corresponding linear terms of the same order of magnitude are also obtained
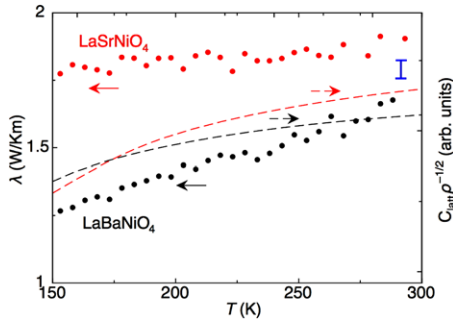
Figure 5. Thermal conductivities $\lambda(T)$ of LaSrNiO$_4$ and oxygen treated LaBaNiO$_4$ (left scale). The dashed lines correspond to $C_{latt}\rho^{-1/2}$, which is related to the lattice contributions λ_{latt}, see text. The solid bar at $T = 290$ K represents the electronic contribution λ_{el} for LaSrNiO$_4$ as estimated from the Wiedemann–Franz law near room temperature.

Table 4. Characteristic parameters for the VRH type conductivity in LaSr$_{0.5}$Ba$_{0.5}$NiO$_4$ and LaBaNiO$_4$.

	LaSr$_{0.5}$Ba$_{0.5}$NiO$_4$		LaBaNiO$_4$	
	2 K	300 K	2 K	300 K
T_0 (K)	1.4×10^4		5.4×10^5	
σ_0 (Ω^{-1} cm^{-1})	100		210	
$D(E_F)$ (J^{-1} m^{-3})	2.1×10^{47}		2.8×10^{47}	
(states eV^{-1}/Ni)	3.1		4.3	
ξ (nm)	0.76		0.21	
R (nm)	2.6	0.75	1.8	0.5
W (meV)	0.40	17	1.0	42
ν (Hz)	2.7×10^{11}	3.4×10^{12}	9.6×10^{11}	1.2×10^{13}
ν_D (Hz)	7.7×10^{12}		6.8×10^{12}	

to be limited by extrinsic, sample dependent parameters at low temperatures. At the same time, the Wiedemann–Franz law that links the thermal conductivity to the electrical conductivity is expected to be valid at high temperatures as well. Therefore we focus on the quantity $C_{latt}\rho^{-1/2}$, which should be proportional to λ_{latt} at a fixed temperature, e.g. at $T = 290$ K. In figure 5 we have plotted the thus obtained $C_{latt}\rho^{-1/2}$ curves for both compounds in such a way that $C_{latt}\rho^{-1/2}$ for LaBaNiO$_4$ approximately matches the measured thermal-conductivity data between 250 and 300 K. If we regard the thermal conductivity of this electrically insulating compound as a pure lattice thermal conductivity, the corresponding calculated $C_{latt}\rho^{-1/2}$ curve for LaSrNiO$_4$ should then represent the lattice contribution of the latter compound as well. This calculated phonon contribution to the thermal conductivity is somewhat smaller than the measured data, however (see figure 5). As LaSrNiO$_4$ shows a metallic electrical conductivity, we may make use of the Wiedemann–Franz law to obtain the electronic contribution to its thermal conductivity, $\lambda_{el} = L\sigma T$ with the Lorenz number $L = 2.44 \times 10^{-8}$ WΩ K^{-2}. Using the room-temperature electrical conductivity $\sigma \approx 90$ Ω^{-1} cm^{-1} we obtain $\lambda_{el} \approx 6.6 \times 10^{-2}$ W K^{-1} m^{-1}, which is of the correct order of magnitude to explain the difference between the measured thermal conductivity and the estimated lattice contribution of LaSrNiO$_4$ near room temperature (see figure 5).

4. Discussion

As a main result of the experimental sections we summarize that LaSrNiO$_4$ and LaBaNiO$_4$ represent two end members of the solid solution LaSr$_{1-x}$Ba$_x$NiO$_4$, in which the transport properties gradually change from metallic-like for $x = 0$ to insulating for $x = 1$. By contrast, the magnetic-susceptibility and the specific-heat data clearly resemble those of a metal, with no apparent difference between LaSrNiO$_4$ and LaBaNiO$_4$. We will first discuss the electrical conductivity alone and show that the variable-range hopping (VRH) scenario is certainly valid to explain the corresponding data for LaSr$_{0.5}$Ba$_{0.5}$NiO$_4$ and LaBaNiO$_4$. We then focus on the magnetic susceptibilities

and the low-temperature specific heats and show that these two quantities are closely related to one another as they are in an ordinary correlated metallic system. We finally briefly discuss a plausible scenario that could explain these seemingly contradictory results.

As we have seen in figure 2(b) the electrical conductivities of LaSr$_{0.5}$Ba$_{0.5}$NiO$_4$ and in particular that of LaBaNiO$_4$ are very well described by a 3D VRH-type temperature dependence $\sigma(T) = \sigma_0 \exp[-(T_0/T)^\alpha]$ with $\alpha = 1/4$ [17]. Other possible exponents such as $\alpha = 1/3$ (2D VRH [17]), $\alpha = 1/2$ (Coulomb-gap T-dependence [19]) or $\alpha = 1$ (activated finite-gap behaviour) result in a considerably worse agreement with the measured data. At first sight, $\sigma(T)$ of the series LaSr$_{1-x}$Ba$_x$NiO$_4$ shown in figure 2(a) strongly resembles the corresponding data measured on heavily doped semiconductors where the slope $|T_0^{1/4}|$ in a $\ln\sigma$ versus $T^{-1/4}$ representation progressively decreases as the system approaches the metal–insulator transition with increasing donor concentration (see, e.g. [20]). However, the physics of LaSr$_{1-x}$Ba$_x$NiO$_4$ is expected to be somewhat different from that of such systems where a number of localized states is supposed to be created within a sizeable band gap of an originally insulating or semiconducting system. Preliminary UV excited photoemission experiments that we have done on LaBaNiO$_4$ clearly exclude the presence of such a band gap that would also manifest itself in an activated (i.e. $\ln\sigma \sim -1/T$) temperature dependence of $\sigma(T)$ at high temperatures, which we do not observe. We can use the same argument to exclude a Mott transition upon stretching the crystal lattice by the substitution of Sr by the larger Ba that would also lead to a band gap. As the VRH conduction mechanism, in its original formulation [17], is not restricted to doped semiconductors but more generally assumes the hopping of electrons in a random potential with localized states, it may nevertheless be a valid description for the conduction mechanism in LaSr$_{1-x}$Ba$_x$NiO$_4$. In the present context we may mention the examples of Li-substituted and oxygen reduced (La, Sr)$_2$CuO$_4$, respectively [21, 22]. While in the former case $T_0 \approx 2 \times 10^6$ K is almost insensitive to the Li-concentration, this quantity increases from ≈ 2000 to $\approx 2 \times 10^5$ K as metallic (La, Sr)$_2$CuO$_4$ is progressively reduced. These values are comparable to what we obtain for LaSr$_{0.5}$Ba$_{0.5}$NiO$_4$ and LaBaNiO$_4$ (see table 4).

To check consistency, we can relate the parameters σ_0 and T_0 from the VRH expression for $\sigma(T)$ to the electron density of states at the Fermi level $D(E_F)$ as measured by the low-temperature specific heat, to the spatial extension ξ of the quasilocalized wavefunction (localization length), to a mean hopping distance R, to the average hopping energy W and to a hopping frequency ν. The quantity $D(E_F)$ can be obtained from the measured Sommerfeld constant using $\gamma = \pi^2 k_B^2 D(E_F)/3$, while $\xi = [18/k_B T_0 D(E_F)]^{1/3}$. The T-dependent R becomes $R = [9\xi/8\pi k_B T D(E_F)]^{1/4}$ and $W = 3/4\pi R^3 D(E_F)$. The hopping frequency $\nu = \sigma_0/e^2 R^2 D(E_F)$ should be, in principle, of the order of a typical phonon frequency, i.e. $\approx \nu_D = k_B \Theta_D/h$ (with e the electron charge and h the Planck constant) where we can use our specific-heat results for the Debye temperatures Θ_D. In table 4 we present the corresponding values that we obtain for $LaSr_{0.5}Ba_{0.5}NiO_4$ and $LaBaNiO_4$.

The values for ν compare reasonably well with our rough estimate for the hopping frequencies, thereby confirming the validity of our approach. As the above relations are valid for an isotropic 3D system, we have to take the values for ξ and R with the reservation that $LaSr_{1-x}Ba_xNiO_4$ is certainly anisotropic. The related system $(La, Sr)_2CuO_4$ shows an anisotropy of the order of 10–20 of the electronically and magnetically relevant length scales in the metallic regime [23], depending on the crystal direction in which they are measured. The 'isotropic' values for ξ may therefore be interpreted in the sense that the true localization lengths along the Ni–O planes are somewhat larger than our calculated ξ, i.e. of the order of a few times the lattice constant a, while the corresponding smaller localization length in the perpendicular direction is most likely only of the size of the extension of the hybridized Ni–O orbitals in the c-direction. The corresponding mean hopping distance is, according to the above estimate, of the same order of magnitude as ξ. The average hopping energies are consistent with the requirement $W \sim k_B T$ to make a hopping to distant sites possible.

From the measured Sommerfeld constants γ given in table 3 we can calculate the density of states at the Fermi level $D(E_F)$ and compare them with the free-electron gas values $D_{f.e.}(E_F) = (3n/\pi)^{1/3} m_e/\pi \hbar^2$ (with the charge-carrier density n, electron mass m_e and $\hbar = h/2\pi$) to obtain the electron effective-mass enhancement $m^*/m_e = D(E_F)/D_{f.e.}(E_F)$. Since we have a nominal $3d^7$ electronic configuration of Ni we may assume here one mobile charge carrier per formula unit to calculate $n = 2/a^2 c$. From $D(E_F)$ and the susceptibility data measured above $T = 40$ K (see table 2) we can also estimate the Stoner enhancement $1/(1-S)$ of the Pauli-paramagnetic susceptibilities using $\chi_0 = 2\mu_B^2 D(E_F)/(1-S)$. In table 5 we show the corresponding values for $LaSrNiO_4$, $LaSr_{0.5}Ba_{0.5}NiO_4$ and $LaBaNiO_4$.

These numbers are all comparable to those that have been measured for metallic $LaNiO_3$ ($\gamma \approx 13$ mJ mol^{-1} K^{-2}, $S \approx 0.58$ [18]) and are usually interpreted as properties of a metal with rather strong electron correlations [4, 18]. Our value for $D(E_F) \approx 4$ states eV^{-1} and the Ni atom for $LaSrNiO_4$ is also in fair agreement with the results from corresponding band-structure calculations for this compound with $D(E_F) \approx 6$ states eV^{-1} [4].

Table 5. Electron density of states, effective-mass and Stoner enhancement from specific-heat and magnetic-susceptibility data.

	$LaSrNiO_4$	$LaSr_{0.5}Ba_{0.5}NiO_4$	$LaBaNiO_4$
$D(E_F)$ (J^{-1} m^{-3})	$2.66(3) \times 10^{47}$	$2.07(5) \times 10^{47}$	$2.81(3) \times 10^{47}$
(states eV^{-1}/Ni)	3.9	3.1	4.3
$D_{f.e.}(E_F)$ (J^{-1} m^{-3})	5.8×10^{46}	5.7×10^{46}	5.7×10^{46}
m^*/m_e	4.62(6)	3.62(8)	4.96(5)
$1/(1-S)$	3.3(1)	4.6(3)	3.2(2)
S	0.70(2)	0.78(5)	0.69(4)

The striking similarity of the low-temperature specific-heat and the magnetic-susceptibility data of $LaSrNiO_4$, $LaSr_{0.5}Ba_{0.5}NiO_4$ and $LaBaNiO_4$ as shown in the figures 3 and 4, with almost identical associated material parameters as summarized in table 5, suggests that the underlying physics that determines these parameters does not significantly change in $LaSr_{1-x}Ba_xNiO_4$ with varying x. This implies that $LaBaNiO_4$ has a finite density of states at the Fermi level, but these states obviously do not contribute to the transport properties, i.e. they must be localized. This situation, together with the observed VRH-type electrical conductivity [17], is very reminiscent of that in a Fermi glass [24–26]. In such a system, the Fermi energy E_F lies below a mobility edge E_c that separates localized electronic states from extended states. The free-electron density of states is then replaced by a quasiparticle density of states, but the expressions for the Sommerfeld constant and the Pauli-paramagnetic susceptibility of the system remain formally the same [25]. Very often E_F can be tuned by changing the charge-carrier concentration to transform an insulating Fermi glass ($E_F < E_c$) to a metal ($E_F > E_c$). At this metal–insulator transition (Anderson transition at $E_F = E_c$), the conductivity at $T = 0$ is expected to be a constant $\sigma(0) = Ce^2/\hbar a$ with $C \approx 0.025$–0.1 [27], which corresponds to $\sigma(0) \approx 160 \cdots 640$ Ω^{-1} cm^{-1} in our case. By comparing this estimate with our results shown in figure 2 we conclude that $LaSrNiO_4$ with $\sigma(0) \approx 90$ Ω^{-1} cm^{-1} is indeed at the borderline of an Anderson-like metal-to-insulator transition. This interpretation is supported by measurements of the electrical conductivity on $La_{2-y}Sr_yNiO_4$ with varying Sr content y, where a finite $\sigma(0) \approx 100$ Ω^{-1} cm^{-1} is measured for polycrystalline samples with $y = 1$ [3] and on thin films at the corresponding metal–insulator transition around $y = 0.95$ [8]. With y decreasing from $y \approx 1$, the resistivity $\rho(T) = \sigma(T)^{-1}$ diverges more and more rapidly as $T \to 0$ according to a VRH-type temperature dependence [8], while increasing y above $y \approx 1$ results in a pronounced metallic behaviour in these measurements [3, 8]. In $LaSr_{1-x}Ba_xNiO_4$ we do not expect to significantly change the charge-carrier concentration, however, because we maintain a formal Ni^{3+} oxidation state, and, as a consequence, our experimental values for $D(E_F)$ virtually do not depend on x. We therefore conclude that the progressive substitution of Sr by Ba increases E_c, rather than changing the charge-carrier concentration or even creating a Mott insulator with a band gap.

In the conventional Anderson metal-to-insulator-transition scenario the magnitude of the mobility edge E_c is determined by the amount of atomic disorder. At first sight it may not be obvious why the isoelectronic substitution of Sr by Ba in $LaSr_{1-x}Ba_xNiO_4$ that is associated with an expansion of the crystal lattice should lead to a growth of such a disorder, with the stoichiometric $LaBaNiO_4$ as the composition with the largest E_c. In a plausible scenario we can relate the atomic disorder to the very large difference between the ionic radii of La and Ba, whereas the respective difference for La and Sr is comparably small. Therefore, atomic disorder is expected to grow with increasing Ba content. However, we want to mention the possibility that charge-localization phenomena that are known to occur in certain other stoichiometric Ni-oxides [15, 16] may also play a certain role in $LaSr_{1-x}Ba_xNiO_4$. In this spirit we can tentatively relate the observed superstructure peaks in our oxygen stoichiometric $LaBaNiO_4$ to such a charge-ordering phenomenon. Whether charge localization alone can lead to a Fermi-glass-type behaviour or not is not known to us. However, such a scenario could well explain that the charge-ordered $La_{2-y}Sr_yNiO_4$ samples for $y \leqslant 0.7$ (see, e.g. [28] and the cited references therein) show a VRH-type electrical conductivity [8, 29], but also a linear term in their low-temperature specific heats ($\gamma \approx$ 10 mJ mol^{-1} K^{-2}) and Pauli-like paramagnetic susceptibilities at high temperatures that are of the order of $\chi_0 \approx 6 \times 10^{-4}$ emu mol^{-1} [29]. These observations, that are very similar to ours, may suggest that an Anderson-like transition is realized in $La_{2-y}Sr_yNiO_4$ around $y \approx 1$, mainly (but perhaps not exclusively) by tuning the Fermi energy with varying y, while in $LaSr_{1-x}Ba_xNiO_4$ it is most likely predominantly the mobility edge that is being tuned.

We conclude that we observe an Anderson-type metal-to-insulator transition in $LaSr_{1-x}Ba_xNiO_4$ around $x \approx 0$ that leads to a Fermi-glass behaviour of $LaBaNiO_4$, with insulating transport properties at $T = 0$ but at the same time with a finite density of states at the Fermi level. We suggest that this transition is caused by an increase of the mobility edge in conjunction with the progressive substitution of Sr by Ba and the increasing atomic disorder associated with it. The insulating state in $LaBaNiO_4$ neither shows antiferromagnetic order nor a finite band gap. We expect that a doping with charge carriers on the moderate level that is sufficient to induce metallic behaviour in the copper oxides (i.e. ≈0.15 holes per transition-metal atom [1]) will not lift the localization of the electronic states in the Fermi-glass state and will therefore not lead to metallic transport properties.

Acknowledgments

References

[1] Bednorz J G and Müller K A 1986 *Z. Phys.* B **64** 189
[2] Jin S, Tiefel T H, McCormack M, Fastnacht R A, Ramesh R and Chen L H 1994 *Science* **264** 413
[3] Cava R J, Batlogg B, Palstra T T, Krajewski J J, Peck W F Jr, Ramirez A P and Rupp L W 1991 *Phys. Rev.* B **43** 1229
[4] Anisimov V I, Bukhvalov D and Rice T M 1999 *Phys. Rev.* B **59** 7901
[5] Kuiper P, Kruizinga G, Ghijsen J, Sawatzky G A and Verweij H 1989 *Phys. Rev. Lett.* **62** 221
[6] van Elp J, Eskes H, Kuiper P and Sawatzky G A 1992 *Phys. Rev.* B **45** 1612
[7] Eisaki H, Uchida S, Mizokawa T, Namatame H, Fujimori A, van Elp J, Kuiper P, Sawatzky G A, Hosoya S and Katayama-Yoshida H 1992 *Phys. Rev.* B **45** 12513
[8] Shinomori S, Okimoto Y, Kawasaki M and Tokura Y 2002 *J. Phys. Soc. Japan* **71** 705
[9] Demazeau G, Marty J L, Buffat B, Dance J M, Pouchard M, Dordor P and Chevalier B 1982 *Mater. Res. Bull.* **17** 37
[10] Alonso J A, Amador J, Gutiérrez-Puebla E, Monge M A, Rasines I, Ruiz-Valero C and Campa J A 1990 *Solid State Commun.* **12** 1327
[11] Demazeau G, Pouchard M and Hagenmüller P 1976 *J. Solid State Chem.* **18** 159
[12] Tranquada J M, Axe J D, Ichikawa N, Nakamura Y, Uchida S and Nachumi B 1996 *Phys. Rev.* B **54** 7489
[13] Chen C H, Cheong S W and Cooper A S 1993 *Phys. Rev. Lett.* **71** 2461
[14] Medarde M and Rodriguez-Carvajal J 1997 *Z. Phys.* B **102** 307
[15] Wawrzynska E, Coldea R, Wheeler E M, Mazin I I, Johannes M D, Sörgel T, Jansen M, Ibberson R M and Radaelli P G 2007 *Phys. Rev. Lett.* **99** 157204
[16] Alonso J A, García-Muñoz J L, Fernández-Díaz M T, Aranda M A G, Martínez-Lope M J and Casais M T 1999 *Phys. Rev. Lett.* **82** 3871
[17] Mott N F 1968 *J. Non-Cryst. Solids* **1** 1
Mott N F 1969 *Phil. Mag.* **19** 835
[18] Sreedhar K, Honig J M, Darwin M, McElfresh M, Shand P M, Xu J, Crooker B C and Spalek J 1992 *Phys. Rev.* B **46** 6382
[19] Shklovskii B I and Efros A L 1984 *Electronic Properties of Doped Semiconductors* (Berlin: Springer)
[20] Shafarman W N and Castner T G 1986 *Phys. Rev.* B **33** 3570
[21] Kastner M A, Birgeneau R J, Chen C Y, Chiang Y M, Gabbe D R, Jenssen H P, Junk T, Peters C J, Picone P J, Tineke T, Thurston T R and Tuller H L 1988 *Phys. Rev.* B **37** 111
[22] Osquiguil E J, Civale L, Decca R and de la Cruz F 1988 *Phys. Rev.* B **38** 2840
[23] Kohout S, Schneider T, Roos J, Keller H, Sasagawa T and Takagi H 2007 *Phys. Rev.* B **76** 064513
[24] Anderson P W 1970 *Comments Solid State Phys.* **2** 193
[25] Freedman R and Hertz J A 1977 *Phys. Rev.* B **15** 2384
[26] Müller K A, Penney T, Shafer M W and Fitzpatrick W J 1981 *Phys. Rev. Lett.* **47** 138
[27] Mott N F 1972 *Phil. Mag.* **26** 1015
[28] Ishizaka K, Arima T, Murakami Y, Kajimoto R, Yoshizawa H, Nagaosa N and Tokura Y 2004 *Phys. Rev. Lett.* **92** 196404
[29] Kato M, Maeno Y and Fujita T 1991 *J. Phys. Soc. Japan* **60** 1994